Phase Transitions in *p*-(Phenyl Benzylidene)-p^1-Alkylaniline Compounds: A Dilatometric Study

Chintalapati Srinivasu[a], Venkata G. K. M. Pisipati[b], Chadalavada R. Prabhu[c],
Piratla Narayana Murty[d], and Somayajula Lakshiminarayana[e]

[a] Department of Physics, Andhra Layola College, Vijayawada-521 008, India
[b] S. S. D. Polymers, Plot No. C-4, APIE, Machilipatnam, India
[c] Faculty of Physics, Department of Applied Sciences, Higher College of Technology, P. O. Box 74, Al-Khwair-133, Muscat, Oman
[d] Department of Physics, Acharya Nagarjuna University, Nagarjunanagar-522 510, India
[e] University Scientific Instrumentation Centre, Acharya Nagarjuna University, Nagarjunanagar-522 510, India

Reprint requests to V. G. K. M. P.; E-mail: venkata_pisipati@hotmail.com

Z. Naturforsch. **62a,** 75 – 83 (2007); received November 6, 2006

Dilatometric studies are carried out on liquid crystals (LCs), viz., *p*-(phenyl benzylidene)-p^1-alkylanilines (PB*n*A for $n = 7 - 10$, 12, 14 and 16). LC PB*n*A compounds are found to exhibit four different types of phase variants. The lower homologues (for $n = 3 - 6$) exhibit an NBE trivariant, intermediate homologues (with $n = 7 - 9$) exhibit an NABE tetravariant, higher homologues (for $n = 10 - 12$) exhibit an ABE tetravariant, and long higher homologues (for $n = 14$ and 16) exhibit an AB bivariant phase sequence. Dilatometry studies in PB*n*A compounds infer the first order nature for IN (for $n = 7$, 8 and 9), IA (for $n = 10$, 12, 14 and 16), NA (for $n = 8$ and 9) and AB (for $n = 14$ and 16) phase transitions. Phase transitions involving the growth of the 3D smectic-B phase in PB*n*As are found to be tuned by squeezing of orientational disorder. A comparative study of phase transitions exhibited by PB*n*A compounds is presented along with the data in other Schiff base compounds.

Key words: Phase Transitions; Dilatometry; Nematic and Smectic Phases; Orientational Disorder.

1. Introduction

In the area of soft-condensed matter physics, the dilatometric investigations of liquid crystal (LC) phase transitions involving different structural organization is an intriguing topic of study. The results of dilatometry are long known [1 – 6] to provide information regarding the nature of the phase transition and the growth of pre-transitional effects. If the dilatometric investigations are carried out in a series of LC compounds (viz., 'systematic studies'), the influence of the molecular structure (i. e., the rigidity/flexibility components of the molecule) on the thermal stability of the LC phases can be studied. Such investigations provide complementary and confirmatory experimental evidence for the results obtained using other techniques [6] like polarization thermal microscopy (TM) and differential scanning calorimetry (DSC) regarding the determination of phase transition temperatures T_C, the nature of the transition and the thermal stability of the phase of interest. *p*-(Phenyl benzylidene)-p^1-alkylaniline (PB*n*A) series of LC compounds are long known [7] to exhibit a variety of polymorphisms, and the abundance of orthogonal LC phases of higher dimensionality due to the presence of an extended rigid core (part of molecular frame). It is noticed that the lower homologues of the PB*n*A series (for $n = 3 - 6$) exhibit [8] a rare sequence of NB phase variance involving a change of dimensionality from one to three. Recent investigations [9] on LC smectic-B phases inferred that a strong molecular inter-locking is tuned by molecular structural parameters (through anti-parallel correlation of longitudinal dipole moments). It is also concluded [10] that the thermal stability of LC smectic-B phases can be tuned by the underlying molecular mobility. The mobility in-turn is discussed in terms of flexibility/rigidity of the molecular frame. It is also noticed [8] that the higher homologues (with long flexible end chains) in an LC series of compounds can effectively induce orientational disorder to account for the LC phase stability. The synthesis, TM and DSC studies are reported [7] in PB*n*A compounds for $n = 3 - 11$, 12 and 15, while their synthesis, TM, DSC and dilatometry are reported [8] for $n = 4 - 6$

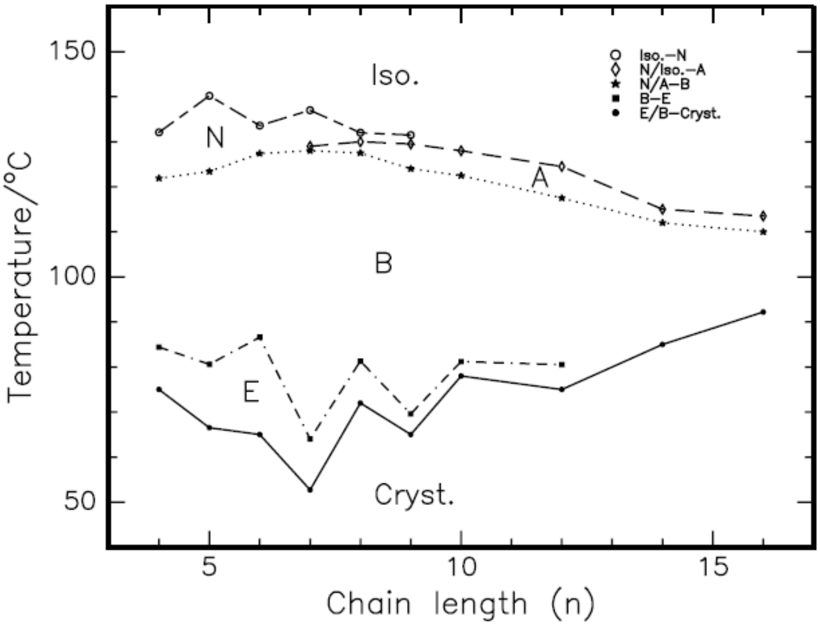

Fig. 1. Phase diagram for PB*n*A series of compounds with details of phase abundance.

compounds only. In the wake of the following aspects of interest,

(i) the LC phase transitions involving a variety of structural organization and
(ii) influence of a long flexible chain in inducing orientational disorder for the phase stability,

we present the results of our dilatometric investigation across the IN, IA, NA, and AB LC phase transitions exhibited by PB*n*A compounds for $n = 7-10$, 12, 14 and 16.

2. Experimental

The PB*n*As were prepared [8] by the condensation of corresponding *p*-*n*-phenyl benzaldehyde (0.1 mol) with the relevant *p*-*n*-alkylaniline (0.1 mol) by refluxing the reactants in absolute ethanol (in the presence of few drops of glacial acetic acid) in cold condition. After refluxing the reactants for 3 – 4 h, the solvent was removed by distillation under reduced pressure. The final compound was re-crystallized from absolute ethanol in cold conditions. Re-crystallization was continued until the transition temperatures were found reproducible. The molecular formula for the LC PB*n*A compound is given by

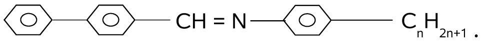

The phase transition temperatures were determined using an Olympus DX50 polarizing microscope equipped with a DP-10 CCD optical display accessory. An Instec temperature controller with an accuracy of ±0.1 K was used to hold the LC microscope slide. A Perkin Elmer DSC-7 instrument was used to determine the transition temperatures and the heats of transition (enthalpy ΔH) involved with them. A U-shaped bi-capillary pycknometer in conjunction with a cathetometer was used during the dilatometry experiments. The absolute error in the measurement of density was $\pm 10^{-4}$ g cm^{-3}. The cooling rate followed during the dilatometry was 0.5 K h^{-1}.

3. Results and Discussion

During the TM studies, the LC phases exhibited (presented in Table 1) by the compounds PB14A and PB16A (synthesized for the first time) are characterized as smectic-A and -B$_{\text{cryst}}$ phases, since they exhibited the standard [11] Schlieren and focal-conic fan textures. The transition temperatures and the associated enthalpy (during heating and cooling runs) determined from calorimetry are presented in Table 1. It is noticed that transition temperatures determined from DSC are found to agree with those from TM. The effect of molecular structure for the LC phase abundance can be studied through a possible comparative qualitative study of phases exhibited by PB*n*A compounds.

Table 1. Transition temperatures (in °C) observed from thermal microscopy (TM) and differential scanning calorimetry (DSC) and dilatometry along with the enthalpy values Δ*H* for PB*n*A compounds.

Compound	Phase variant	Method		IN/A	NB/A	AB	BE	B/EK	Ref.
PB4A	NBE	DSC	Cooling	132.11	121.90				
			Δ*H* (J/g)	1.27	25.85				
		TM	Cooling	132.10	121.90		85.40	75.00	
		Density	Cooling	132.00	121.80				
PB5A	NBE	DSC	Cooling	140.20	123.40				
			Δ*H* (J/g)	1.62	22.12				
		TM	Cooling	140.20	123.40		80.60	66.50	[7]
		Density	Cooling	140.20	123.40				
PB6A	NBE	DSC	Cooling	133.50	127.50				
			Δ*H* (J/g)	1.41	24.25				
		TM	Cooling	133.60	127.4		86.58	65.00	
		Density	Cooling	133.50	127.4				
PB7A	NABE	DSC	Heating	135.98	130.88	130.01		83.45	
			Δ*H* (J/g)	2.08	0.63	2.98		63.60	
			Cooling	135.90	127.20	125.90	56.72	52.67	
			Δ*H* (J/g)	1.87	2.15	92.89	0.84	49.88	
		TM	Cooling	137.00	129.00	128.00	64.00		
		Density	Cooling	136.00	127.20	126.40			
PB8A	NABE	DSC	Heating	134.53	132.21	130.00		95.05	
			Δ*H* (J/g)	1.25	4.80	8.21		76.02	
			Cooling	131.37	128.08	125.46	79.20	61.64	
			Δ*H* (J/g)	1,99	5.70	9.68		72.21	
		TM	Cooling	132.00	130.00	127.50	81.30	90.00	
		Density	Cooling	131.40	128.00	125.60			
PB9A	NABE	DSC	Heating	133.89	131.37	126.14		91.23	
			Δ*H* (J/g)	2.06	5.26	9.84		68.09	
			Cooling	132.50	129.80	124.40	68.20	65.60	
			Δ*H* (J/g)	2.00	5.10	9.50		45.20	
		TM	Cooling	131.50	129.50	124.00	69.80	86.00	
		Density	Cooling	132.60	129.80	124.40			
PB10A	ABE	DSC	Heating	130.78		124.82		99.73	
			Δ*H* (J/g)	10.79		9.55		92.83	
			Cooling	128.55		122.83	80.10	78.52	
			Δ*H* (J/g)	6.77		6.74		94.07	pw
		TM	Cooling	128.00		122.50	81.20	92.00	
		Density	Cooling	128.60		123.90			
PB12A	ABE	DSC	Heating	128.68		121.50		105.40	
			Δ*H* (J/g)	13.33		11.95		124.75	
			Cooling	124.44		117.37	80.00	75.50	
			Δ*H* (J/g)	13.58		11.64		122.28	
		TM	Cooling	124.50		117.50	80.50	98.0	
		Density	Cooling	124.60		117.50			
PB14A	AB	DSC	Heating	124.59		116.89		108.95	
			Δ*H* (J/g)	8.17		8.33		102.75	
			Cooling	120.91		113.33		85.32	
			Δ*H* (J/g)	9.1		7.70		53.80	
		TM	Cooling	115.00		112.00		99.00	
		Density	Cooling	121.10		113.50			
PB16A	AB	DSC	Heating	118.56				110.85	
			Δ*H* (J/g)	9.57				119.75	
			Cooling	116.11		108.88		92.61	
			Δ*H* (J/g)	6.48		7.76		117.46	
		TM	Cooling	113.50		110.00		106.00	
		Density	Cooling	116.20		108.80			

pw, present work.

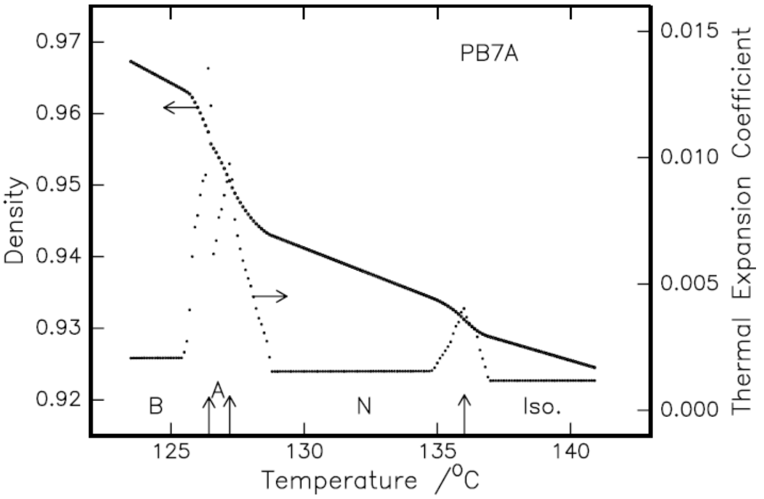

Fig. 2. Temperature variation of density $\rho(T)$ and thermal expansion coefficient $\alpha(T)$ for PB7A compound.

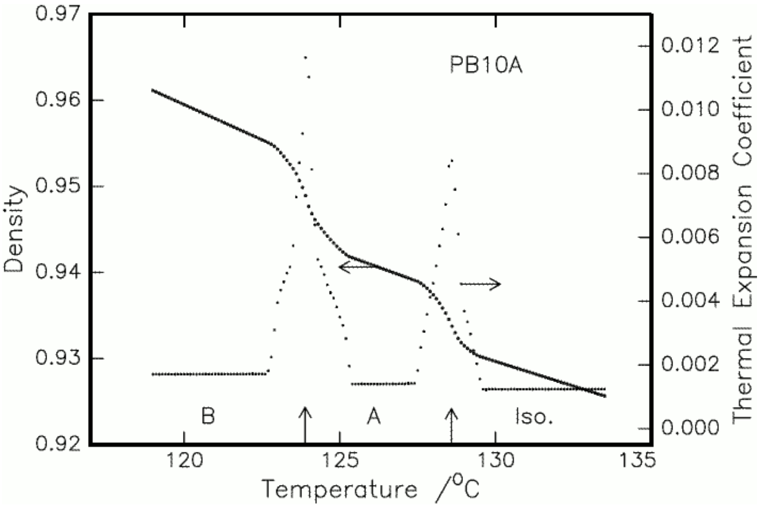

Fig. 3. Temperature variation of density $\rho(T)$ and thermal expansion coefficient $\alpha(T)$ for PB10A compound.

The details of LC phases and transition temperatures reported [7, 8] (for $n = 3-12$ and 15) along with that of the present work (for $n = 14$ and 16) are presented in the form of a phase diagram (Fig. 1) for the comparative study in the LC PB*n*A series of compounds. As such, a meticulous study of the phase diagram is expected to reveal the influence of flexible/rigid components of the molecular frame for the thermal stability of the phases exhibited by the PB*n*A series.

An overview of Fig. 1 drawn for PB*n*A compounds, readily reckons the fact that the clearing temperatures and the melting temperatures observed in the PB*n*A series of compounds follow and odd-even effect. It is also noticed from Fig. 1 that the trend of the odd-even effect (in the lower homologues) gets decreased to a minimum with the increase of n in the PB*n*A series. This trend of reduced odd-even effect is argued [12] as due to the induced orientational disorder with the increasing chain length. In fact, the increasing flexibility is found to smoothly tune the contributions of axial polarizabilities, as discussed in Marcelja's model [13].

An overview of the present work (for $n = 14$ and 16 in Table 1) and that reported [7, 8] on other PB*n*A compounds along with that presented in Fig. 1, reveals that the PB*n*A series of compounds exhibits

(i) a tetravariant NABE phase sequence in lower (for $n = 3-7$) homologues;
(ii) a trivariant NBE phase sequence in intermediate (for $n = 7-9$) homologues;
(iii) a tetravariant NABE phase sequence in higher (for $n = 9-12$) homologues;

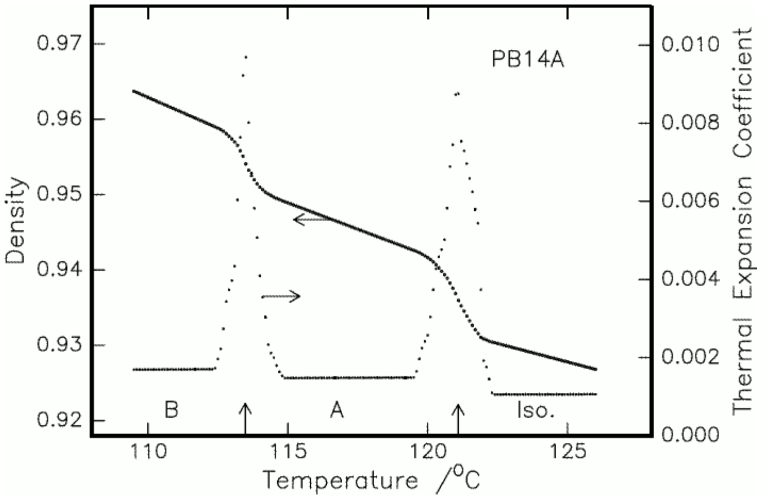

Fig. 4. Temperature variation of density $\rho(T)$ and thermal expansion coefficient $\alpha(T)$ for PB14A compound.

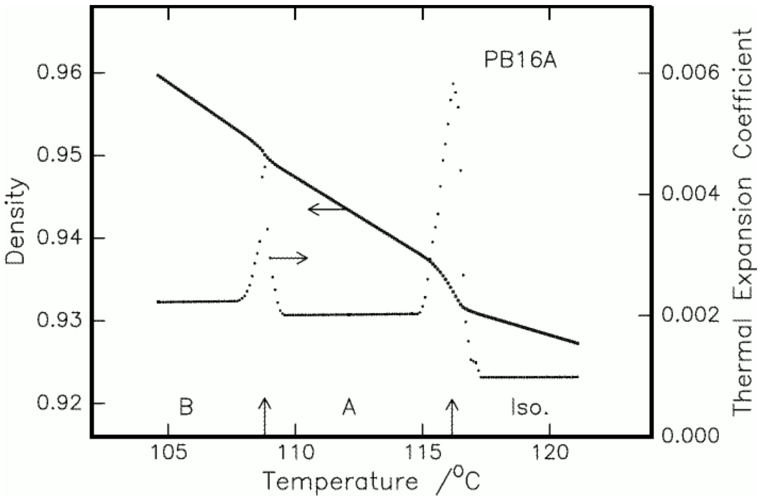

Fig. 5. Temperature variation of density $\rho(T)$ and thermal expansion coefficient $\alpha(T)$ for PB16A compound.

(iv) a bivariant AB phase sequence in very long (for $n = 13-16$) homologues.

As such, it may be argued that the orthogonal 3D smectic-B and smectic-E LC phases are quenching the nematic phase with increase of the flexible end chain component of the molecule. Further, the higher homologues (PB14A and PB16A) are found to exhibit smectic-A and -B phases only. This implies that a further increase of the chain length n (i. e., $n = 14$ and 16) may possibly result in quenching of smectic-E phase also. Thus, the quenching of the nematic and smectic-E phase with increase of n is interpreted as due to increased orientational disorder (or the flexible part of the molecule). In summary, the orientational disorder is found to be prevalent in the higher homologues.

It is noticed that the experimental investigations reported for PB*n*A compounds [7], for $n = 3-6$ inferred an NBE phase variance. Hence, in the present work we carried out dilatometry of the remaining PB*n*A compounds, exhibiting NABE, ABE, and AB phase variance (i. e., compounds for $n = 7$ and 8, 9 – 12 and 13 – 16, respectively). The density plots for NABE variance (for $n = 7$ as representative) is presented in Fig. 2, while that for ABE phase variance (for $n = 10$) is presented in Figure 3. However, the density plots for AB variance (for $n = 14$ and 16) are presented in Figs. 4 and 5.

The observed temperature variations of the density $\rho(T)$ and the thermal expansion maxima $\alpha(T)$ for the compounds PB7A, PB10A, PB14A and PB16A are presented in Figs. 2 – 5, respectively. It may be noticed that the density variations for the compounds $n = 7$ and 10 are only presented, since they are capable of representing NABE and ABE phase variants exhibited by the PB*n*A series [7]. The density is found to increase linearly with decreasing temperature in the equilibrium LC phases, while it is found to increase nonlinearly in the vicinity of phase transitions. The volume expansion coefficient is found to be constant in the equilibrium LC phases and exhibits a peak value at the transition point. The phase transition temperatures determined from density measurements are demarcated as inset arrows in Figures 2 – 5. The transition temperatures determined from dilatrometry (presented in Table 1) are found to agree [7, 8] with TM and DSC values.

The density jumps ($\Delta\rho/\rho$) are estimated from the difference ($|\rho_1 \sim \rho_2| = \Delta\rho$) between the (linearly) extrapolated density values ρ_1 and ρ_2 (from either sides of the transitions) and their average density $[(\rho_1 + \rho_2)/2 = \rho]$ value at the transition. The thermal expansion coefficient α is estimated from the equation

$$\alpha(T) = (1/M_\text{V})(\text{d}M_\text{V}/\text{d}T), \tag{1}$$

where M_V is the molar volume.

The estimated molar volume M_V in the isotropic phase for the compounds PB7A, PB8A, PB9A, PB10A, PB12A, PB14A and PB16A at $T_{\text{I-N/A}}$ plus 5 °C are found to be 384.6, 399.5, 414.6, 429.6, 459.6, and $489.6 \cdot 10^{-6}$ m^3 mol^{-1}, respectively. The increment in M_V per n (i. e., methyline unit) estimated in the isotropic liquid phase in the LC PB*n*A series is found to be slightly smaller than that reported in [6, 12, 14] for normal isotropic liquids. However, the values in the present PB*n*A compounds are found to agree with those reported in [8] for lower homologues.

3.1. Isotropic-Nematic (IN) Transition

The slopes of density with temperature $\text{d}\rho/\text{d}T$, in the equilibrium isotropic phase of the PB7A, PB8A, PB9A, PB10A, PB12A, PB14A and PB16A compounds are found to be 10.90, 15.36, 8.30, 11.45, 14.0, 9.8, $9.1 \cdot 10^{-4}$ g cm^{-3} K^{-1}, respectively. The observed $\text{d}\rho/\text{d}T$ values are found to agree with those reported [15] for *n*O.*m* compounds. The observed higher values of the slopes of the density (in the equilibrium regions) in the nematic phase exhibited by these compounds (14.5, 24.5, and $14.5 \cdot 10^{-4}$ g cm^{-3} K^{-1}) are indicative of an increase in the molecular packing in the nematic phase. The observed increase also infers the growth of long range orientation order. The thermal expansion coefficient maxima obtained for these compounds are found to agree [8] with the body of the data reported in the literature. The isotropic-nematic (IN) transitions observed in PB7A, PB8A and PB9A are accompanied by density jumps ($\Delta\rho/\rho \cdot 100$) of 0.38, 0.30 and 0.41, and the thermal expansion coefficient maxima of $40.1 \cdot 10^{-4}$ K^{-1}, $67.2 \cdot 10^{-4}$ K^{-1}, $76.8 \cdot 10^{-4}$ K^{-1}, respectively (Table 2). The finite density jumps and the thermal expansion coefficient maxima in these compounds infer the isotropic to nematic transition to be of first order. The $\Delta\rho/\rho$ across the IN transition in PB*n*A compounds are found to be consistent with the body of data reported on LC *n*O.*m* compounds [16]. Although, the density jumps observed at the IN transition for the present (Table 2) PB*n*A compounds (PB7A, PB8A and PB9A) are found to be relatively smaller than those reported for *n*O.*m* (5O.9 [17], 7O.1 [18] and 5O.10 [19]) compounds, they are found to agree with the values obtained for the lower homologues of PB*n*A compounds [7]. It is also noticed that the present values of $\Delta\rho/\rho$ in PB*n*A compounds are found to be smaller than the general limiting (0.4 to 0.5%) values proposed by Grasso et al. [20]. The observed small, but distinct jumps across the IN transition for all these compounds reflect a relatively disordered state of the nematic phase. As such, a PB*n*A molecule is inferred to possess a relatively small orientation potential barrier across the IN transition.

The pressure dependence of the IN transition temperature, $\text{d}T_\text{IN}/\text{d}p$, is estimated by the Clausius-Clapeyron equation

$$(\text{d}T_\text{C}/\text{d}p) = T_\text{C} * (\Delta M_\text{V}/\Delta H), \tag{2}$$

where T_C is the transition temperature (i. e. T_IN in our case) and ΔM_V is the estimated change in molar volume at the IN transition. The $\text{d}T_\text{IN}/\text{d}p$ data estimated from the density and the DSC data are for PB7A, PB8A and PB9A presented in Table 2. The values of pressure dependence T_IN are found to agree with the values reported for other PB*n*A compounds [8].

3.2. Nematic to Smectic-A (NA) Transition

The nematic to smectic-A (NA) transition in compound PB7A could not be visualized during the cooling of the sample due to the very narrow thermal span of the smectic-A phase (higher side of the NA transition). However, the NA transition is found to be accompanied by a thermal expansion coefficient maximum in

Table 2. Details of phase variants, density jumps $\Delta\rho/\rho$, thermal expansion coefficient maxima $\alpha_{\max}(T)$ and the pressure dependence of the transition temperatures $\mathrm{d}T_\mathrm{c}/\mathrm{d}p$ for the members of PB*n*A series of compounds.

Compound	Phase	$\Delta\rho/\rho \times 100$			$\alpha_{\max} \times 10^{-4}$ K^{-1}			$\mathrm{d}T_\mathrm{C}/\mathrm{d}p$ (K kbar^{-1})			Ref.
	variant	IN/A	NB/A	AB	IN/A	NB/A	AB	IN/A	NB/A	AB	
PB4A	NBE	0.18	1.66		25.0	246.0		59.4	27.1		[7]
PB5A	NBE	0.26	1.61		22.0	219.0		71.1	30.7		
PB6A	NBE	0.21	1.73		28.0	267.0		70.6	30.3		
PB7A	NABE	0.38	–	1.62	40.1	97.4	136.0	81.7	–	68.6	pw
PB8A	NABE	0.30	0.73	0.68	67.2	107.6	106.0	65.9	23.3	29.2	
PB9A	NABE	0.41	0.45	0.71	76.8	80.0	158.0	95.5	37.0	30.8	
PB10A	ABE	0.70		1.06	84.0		117.0			65.9	
PB12A	ABE	1.17		0.75	96.0		69.0			26.4	
PB14A	AB	1.10		0.63	88.0		97.0			30.7	
PB16A	AB	0.36		0.11	58.0		45.0			5.4	

pw, present work.

the form of a shoulder (in Fig. 2) on the higher temperature side of the smectic-A to smectic-B transition. The NA transition in PB8A and PB9A compounds is found to be accompanied by a density jump of 0.73%, and 0.45%. The $\alpha_{\max}$ values are $107.6 \cdot 10^{-4}$ K^{-1} and $80.2 \cdot 10^{-4}$ K^{-1}, respectively. The density jumps and $\alpha_{\max}$ values across the NA transition in PB*n*A compounds are found to be slightly higher than those reported for LC *n*O.*m* compounds [16]. The observed finite density jump and the α values suggest that the NA transition is of first order in PB*n*A compounds. The occurrence of a first order NA transition in PB*n*A compounds is found to agree with the prediction of McMillan's theory. The McMillan parameter, $M = T_\mathrm{NA}/T_\mathrm{NI}$, is found to be 0.977, 0.991 and 0.993 for the PB7A, PB8A and PB9A compounds, respectively. These values are found to be far higher than the value of 0.87, to predict the first order nature of a NA transition [21]. It is also noticed that the ΔH values observed across an NA transition [7, 8] are rather large. The large $T_\mathrm{NA}/T_\mathrm{IN}$ and ΔH values observed in the PB*n*A series across an NA transition are argued as due to contributions of pretransitional effects. A similar trend of a higher McMillan parameter (i.e., > 0.959) is found to be reported for first order NA transitions in LC *n*O.*m* compounds [22].

The slopes of density plots estimated in the equilibrium smectic-A phase $(\mathrm{d}\rho/\mathrm{d}T)_\mathrm{A}$ in PB7A, PB8A and PB9A are found to be 20.7, 27.0 and $19.0 \cdot 10^{-4}$ g cm^{-3} K^{-1}, respectively. The observed higher slopes of density plots in the smectic-A phase (than those in the nematic phase) are argued as due to the growth of layering order in addition to the orientational order.

The pressure dependence of the NA transition temperature $\mathrm{d}T_\mathrm{NA}/\mathrm{d}p$, estimated from the density data and DSC (Table 2) using the Clausius-Clapeyron equation, is found to be 23.3 and 36.9 K kbar^{-1} for PB8A and PB9A, respectively. However, the pressure dependence of the NA transition temperature in the case of PB7A could not be estimated because of the narrow thermal range of the smectic-A phase and the paucity of the density data to resource the NA and AB transition. The pressure dependence of the NA transition for PB8A and PB9A is found to agree with the values reported [23] for 6O.8. However, the observed variance of value for $\mathrm{d}T_\mathrm{NA}/\mathrm{d}p$ among various compounds is attributed to factors like the difference in experimental techniques used, scanning rates employed and the molecular systems used during the experiments.

3.3. Isotropic to Smectic-A (IA) Transition

The density jumps observed across the isotropic to smectic-A (IA) transition in the present PB*n*A compounds along with the thermal expansion coefficient maxima ($\alpha_{\max}$) are presented in Table 2. They are found to agree with the reported values in other *n*O.*m* [16] and in the TB*n*A series [24] of compounds. The slopes of density in the equilibrium smectic-A phase, i. e. $[\mathrm{d}\rho/\mathrm{d}T]_\mathrm{IA}$ in the PB*n*A compounds for $n = 10$, 12, 14 and 16 are 13.15, 14.8, 14.0 and $18.9 \cdot 10^{-4}$ g cm^{-3} K^{-1}, respectively. These values are found to agree with the reported [25] values in other LC *n*O.*m* compounds. The higher values of the slopes of density plots in the smectic-A phase than those in the isotropic phase are indicative of denser packing of the molecules.

The IA transition is observed (Table 2) to be accompanied by large density jumps of 0.70, 1.17, 1.10, and 0.36% for the PB10A, PB12A, PB14A and PB16A compounds, respectively. The large density jump across the IA transition is argued as due to the simultaneous growth of orientational order and periodic translational order (layered arrangement of molecules) from the completely disordered isotropic liquid. The finite values of density jumps and thermal expansion coefficient maxima in these compounds indicate the first order nature of IA phase transitions.

Dilatometry studies across the IA transition are found to accompany a large fluctuation dominated nonlinear region (FDNLR, to a maximum of ≈ 1.5 K) in these compounds. Nevertheless, the visual observations across IA transitions reveal the growth of translucent smectic-A phase at the bottom of the pycknometer bulb, while transparent isotropic liquid floats over it with a clear separating boundary between them. On further cooling of the sample, the translucent smectic-A phase is found to permeate through the isotropic liquid in the pycknometer bulb. The formation of smectic-A embryos first at the bottom of the bulb, and their subsequent spread upwards clearly indicates the 'nucleation' type of growth during the IA phase transition. Further, the range of density jumps observed (Table 2) across the IA transition in the present compounds are found to fall in between the maximum and minimum values reported for *n*O.*m* compounds [25, 26]. It is noticed that the density jump of 0.36% and $58.2 \cdot 10^{-4}$ K^{-1} across this transition in PB16A is found to be small and indicative of a relatively small potential barrier. The small potential barrier is argued as due to the possible orientational disorder induced [6] by the flexible end chain in the higher homologues of LC compounds.

The estimated pressure dependence of transition temperature at the IA transition, $\mathrm{d}T_{\mathrm{IA}}/\mathrm{d}p$ using the Clausius-Clapeyron equation and the experimental data (from calorimetry and dilatometry as presented in Table 2) are found to agree [8, 12] with the reports on other LC compounds.

3.4. Smectic-A to Smectic-B$_{cryst}$ (AB) Transition

Microscopic textural observations revealed that further cooling of the smectic-A phase results in the appearance of transient transition bars across the smectic-A focal-conic fans at the transition. However, these bars disappear on further cooling with the formation of smooth focal conic fans with a reduced number of discontinuities (on the edges of the domains). The observed density jumps and the thermal expansion coefficient maxima for the PB*n*A compounds across the AB transition are presented in Table 2. Further, the observed density increase across the AB transition is not found to be a step function similar to that reported across the CB transition [12, 27]. The AB transition in the present compound is observed as a linear increment from the smectic-A to the smectic-B phase with a finite slope. Further, the presence of a two-phase coexistence (for a small temperature range) is also observed, which is found to co-terminate with simultaneous broadening of transition. Hence, the observed broadening is attributed to the existence of a phase coexistence region. It may also be reckoned that this common occurring of LC phase coexistence phenomena does not require any vestiges of pre-transitional effects (observed during CB transition). On the other hand, as the AB transition involves the growth of positional ordering in the smectic-B phase from the layered molecular arrangement of the smectic-A phase, the occurrence of two-phase coexistence is justified. Although it is conceivable that the trace level impurities might have converted the otherwise second order AB transition to the observed first order transition, there is absolutely no evidence to believe that this impurity broadening phenomenon is occurring here. In fact, the absence of pre-transitional phenomena (exclusively expected for second or weakly first order transitions) weighs heavily against any such hypothesis here.

Although the density jumps across the AB transition are found to exhibit an odd-even effect, the observed decreasing trend in their magnitudes with the increase of the alkyl chain (i. e., increasing value of *n* in the PB*n*A series) is found to be interesting. Further, the odd-even effect is known [13] to contribute anisotropic axial polarizabilities. Hence, these contributions seem to be effectively squeezed at the interface, involving the growth of a 3D smectic-B phase.

The crystalline smectic-B phase has a long-range three-dimensional order with positional correlation of hexagonal in-plane packing of molecules as well as layers. As such, the AB transition is expected to be of first order nature. Finite density jumps of 1.62, 0.68, 0.71, 1.06, 0.75, 0.63, and 0.11% and the thermal expansion coefficient maxima $\alpha_{\max}$ of 136.0, 106.0, 158.0, 117.0, 69.0, 97.0, and $45.0 \cdot 10^{-4}$ K^{-1} are found to be accompanied by the AB transition for PB7A, PB8A, PB9A, PB10A, PB12A, PB14A, and PB16A, respectively. These values indicate that the AB transition in PB*n*A compounds is of first order nature. On further cooling of a sample in its smectic-B phase, results in the loss of continuity in the columns of the pycknometer and breaks occur in the sample. The observed breaks infer an increase of viscocity in the smectic-B phase with decreasing temperature.

The pressure dependence T_{IA} (estimated from the density and calorimetric data using the Clausius-Clapeyron equation) for the PB7A, PB8A, PB9A, PB10A, PB12A, PB14A and PB16A compounds (Table 2) is found to be comparable to that reported [16, 28] across the AB transition in LC *n*O.*m* compounds.

4. Conclusions

1.) The dilatometry studies on PB*n*A compounds (with the alkyl chain length $n = 7-10$ and 12, 14 and 16) reveal that the IN, IA, NA and AB transitions are of first order nature.

2.) The decreasing density jumps (in higher homologues) with increasing flexible chain length reflects a smaller potential barrier across the AB transition. Hence it is concluded that an orientational potential barrier is effectively tuned by the induced orientational disorder.

3.) The decreasing odd-even effect (with increasing chain length for the density jumps across the AB transition) with increasing chain length (as contributions of axial polarizabilities) reflects the effective squeezing of orientational disorder at the phase transitions involving an LC smectic-B phase.

Acknowledgements

C. Srinivasu acknowledges the financial support provided by U. G. C., New Delhi during his FIP program.

[1] V. A. Burmistrov, A. V. Zavyaloy, I. V. Novikoy, S. A. Kuvshinova, and V. V. Aleksandriskii, Russ. J. Phys. Chem. **79**, 130 (2005).
[2] B. Gogoi, T. K. Ghosh, and P. R. Alapati, Cryst. Res. Tech. **40**, 709 (2005)
[3] N. Ajeetha, M. Ramakrishna Nanchara Rao, P. V. Datta Prasad, and V. G. K. M. Pisipati, Z. Naturforsch. **60a**, 746 (2005).
[4] N. Ajeetha, M. Ramakrishna Nanchara Rao, P. V. Datta Prasad, and V. G. K. M. Pisipati, Mol. Cryst. Liq. Cryst. **452**, 3 (2006).
[5] B. Gogoi, P. R. Alapati, and A. L. Verma, Cryst. Res. Techn. **37**, 1331 (2002).
[6] S. Padmaja, M. Ramakrishna Nanchara Rao, P. V. Datta Prasad, and V. G. K. M. Pisipati, Z. Naturforsch. **60a**, 296 (2005).
[7] J. J. Benattar, A. M. Kevkyt, and L. Strazelecki, J. Phys. (Paris) **39**, 1233 (1978).
[8] D. M. Potukuchi, S. Lakshiminarayana, and V. G. K. M. Pisipati, Cryst. Res. Tech. **31**, 685 (1996).
[9] B. Benguigui, Phys. Rev. A **28**, 1852 (1983).
[10] B. Bahadur, B. K. Sarna, A. K. Garg, and V. K. Agarwal, Mol. Cryst. Liq. Cryst. **100**, 137 (1983).
[11] G. W. Gray and J. W. Goodby, in: Smectic Liquid Crystals, Textures and Structures, Leonard Hill, London 1994.
[12] N. V. S. Rao, D. M. Potukuchi, and V. G. K. M. Pisipati, Mol. Cryst. Liq. Cryst. **196**, 71 (1991).
[13] S. Marcelja, J. Chem. Phys. **60**, 3599 (1974).
[14] I. H. Haller, H. A. Huggins, H. R. Lillenthal, and T. R. McGuire, J. Phys. Chem. **24**, 950 (1973).
[15] N. V. S. Rao and V. G. K. M. Pisipati, J. Phys. Chem. **87**, 899 (1983).
[16] C. R. Prabhu and V. G. K. M. Pisipati, Cryst. Res. Tech. **37**, 269 (2002).
[17] V. G. K. M. Pisipati, N. V. S. Rao, M. V. V. Nagi Reddy, C. G. Rama Rao, and G. Padmavati, Cryst. Res. Tech. **26**, 709 (1991).
[18] N. V. S. Rao, P. V. Datta Prasad, and V. G. K. M. Pisipati, Mol. Cryst. Liq. Cryst. **126**, 175 (1985).
[19] N. V. S. Rao, P. V. Datta Prasad, V. G. K. M. Pisipati, and P. R. Alapati, Phase Transitions **5**, 187 (1985).
[20] D. Grasso, S. Fasone, G. Dipasquale, and F. Cospelli, Thermochim. Acta **140**, 31 (1989).
[21] V. G. K. M. Pisipati, N. V. S. Rao, and P. R. Alapati, Cryst. Res. Techn. **24**, 1285 (1989).
[22] S. B. Rananavare, V. G. K. M. Pisipati, and J. H. Freed, Chem. Phys. Lett. **140**, 235 (1987).
[23] V. G. K. M. Pisipati, N. V. S. Rao, M. K. Rao, D. M. Potukuchi, and P. R. Alapati, Mol. Cryst. Liq. Cryst. **146**, 89 (1987).
[24] S. Lakshminarayana, C. R. Prabhu, D. M. Potukuchi, N. V. S. Rao, V. G. K. M. Pisipati, Liq. Cryst. **20**, 177 (1996).
[25] N. V. S. Rao, D. M. Potukuchi, P. V. Sankara Rao, and V. G. K. M. Pisipati, Liq. Cryst. **12**, 127 (1992).
[26] V. G. K. M. Pisipati, J. S. R. Murthy, N. V. S. Rao, and Y. G. Sankar, Acoustica **60**, 163 (1986).
[27] N. V. S. Rao, V. G. K. M. Pisipati, Y. Gouri Sankar, and D. M. Potukuchi, Phase Transitions **7**, 49 (1986).
[28] C. R. Prabhu, S. Lakshiminarayana, and V. G. K. M. Pisipati, Z. Naturforsch. **59a**, 537 (2004).